

The geochemistry and geochronology
of igneous bodies intersected in
Nankivel Core PPDH155

Thesis submitted in accordance with the requirements of the University of
Adelaide for an Honours Degree in Geology

Benjamin John Blaschek
November 2017



THE UNIVERSITY
of ADELAIDE

GEOCHEMISTRY AND GEOCHRONOLOGY OF IGNEOUS BODIES INTERSECTED IN NANKIVEL CORE PPDH155

GEOCHEMISTRY AND GEOCHRONOLOGY OF PPDH155

ABSTRACT

The Gawler Craton is host to regions of high economic significance these are the Central Gawler Gold Province and the Olympic Iron Ore Copper Gold Province with both of these regions being related to Mesoproterozoic igneous bodies primarily from the Hiltaba Suite (1595-1575Ma). As such being able to understand the geochemistry and formational conditions of the igneous bodies is of high importance to both science and industry. This paper pertains to Mesoproterozoic igneous bodies with a range of compositions intersected by Investigator Resources PPDH155 Nankivel core located within the Central Gawler Gold Province. Geochemical and Geochronological analysis was undertaken on samples from the Hiltaba Suite and samples from PPDH155 with supporting data from existing literature on the St Peter Suite (1620-1608Ma) to attempt to determine the age and formational conditions of the magmatic bodies intersected within the drill core. From this analysis age dates of 1577 \pm 24Ma and 1624 \pm 38Ma were obtained for samples from PPDH155 with geochemistry which more closely resembles that of the Hiltaba Suite. However, the data also suggests that the formational processes which led to the development of these igneous bodies are quite complex and further investigation is required to produce a more detailed understanding of these processes.

KEYWORDS

Geochemistry
Geochronology
Igneous geology
Mesoproterozoic
Gawler Craton
Hiltaba Suite
St Peter Suite

TABLE OF CONTENTS

geochemistry and geochronology of igneous bodies intersected in Nankivel Core
PPDH155 i

Geochemistry and Geochronology of PPDH155..... i

Abstract..... i

Keywords..... i

List of Figures and Tables 2

Introduction 3

Geological Setting 7

Methods 8

observations and Results 11

Discussion..... 17

Conclusions 21

Acknowledgments 22

References 23

Appendix A: Core Photographs..... 1

LIST OF FIGURES AND TABLES

Figure 1: Map showing the spatial extent and relationships of the Gawler Craton metalliferous regions as well as their relationship between rock units, heat flow, structural features, and mining ventures (Hand, Reid, & Jagodzinski, 2007).	3
Figure 2: Sample locations with the Green star representing the Nankivel drill core.....	4
Figure 3: core log and petrographical observations	11
Figure 4: PPDH155 Core photos and thin section photomicrographs. 4a) Core photo of 60.3m – 66.99m segment containing sample 436024 which is the most mafic sample with silica of 55.4%. 4b) Core photo of 312.52m – 321.26m segment containing sample 436006 which is an intermediate sample with silica of 64.6%. 4c) Core photo of 107.71m – 114.51m segment containing sample 436023 which is the most felsic sample with silica of 69.5%. 4d) Photomicrograph of cross polarised sample at 369.7m showing potassic alteration of quartz monzodiorite with relict biotites as large red/brown plates. 4e) Photomicrograph of cross polarised sample at 247.47m – 247.80m showing granitoid wall rock fragment hosted in breccia, granite is to the bottom right of the image.	12
Figure 5: IUGS output from GCDkit using the TAS system from Middlemost 1985 (J. B. H, 2009)	13

INTRODUCTION

The Gawler craton, South Australia is host to two large metalliferous provinces linked to magmatic events that coincide with the emplacement of the 1595 Ma to 1575 Ma Hiltaba Suite. These regions are of high interest to industry and understanding the formation and emplacement conditions of the magmatic bodies which lead to their formation is of high importance to both industry and earth scientists due to the high level of economic significance associated with these provinces. The two metalliferous regions found within the Gawler Craton are the Central Gawler Gold Province and the Olympic Iron Ore Copper Gold Province. These proposed provinces are shown in figure 1 (Hand, Reid, & Jagodzinski, 2007).

The emplacement of the Hiltaba Suite aged magmatic bodies is believed to have been a major driver in the formation of economic deposits within the region and are potentially the source material for the metals or as mobilising agents with crustal scale thermal and fluid flow events occurring synchronously with emplacement. As such constraining the emplacement ages of these magmatic bodies and determining the geochemical relationship between the individual bodies can give insights into the Mesoproterozoic development of these crustal events and their link to the formation of the two metalliferous regions with a focus on the formational differences between the IOCG

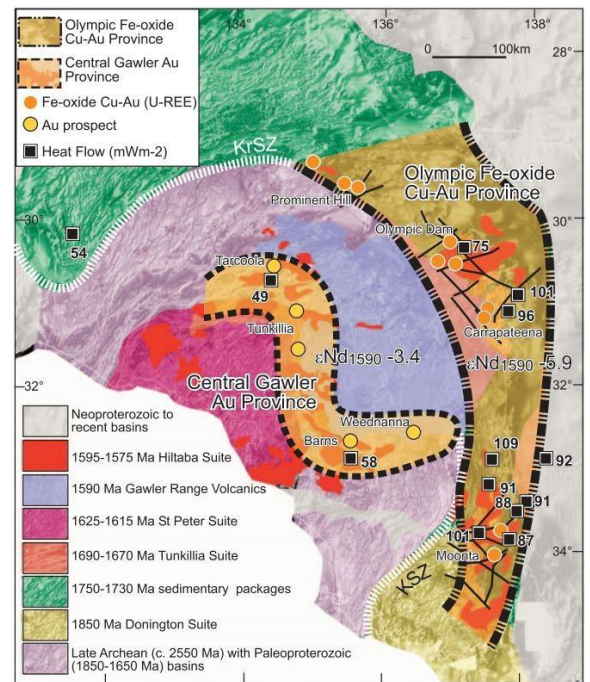


Figure 1: Map showing the spatial extent and relationships of the Gawler Craton metalliferous regions as well as their relationship between rock units, heat flow, structural features, and mining ventures (Hand, Reid, & Jagodzinski, 2007).

region and the Central Gawler Gold Province. It has been proposed that the key difference is the presence of mafic bodies within the IOCG province in association with the granitic bodies. Conversely the Central Gawler Gold Province shows a comparatively low amount of mafic involvement and a much higher contribution from granitic bodies and alteration with a spatial and temporal relationship to these granites.

Sample Locations of Nankivel, St Peter Suite and Hiltaba Suite

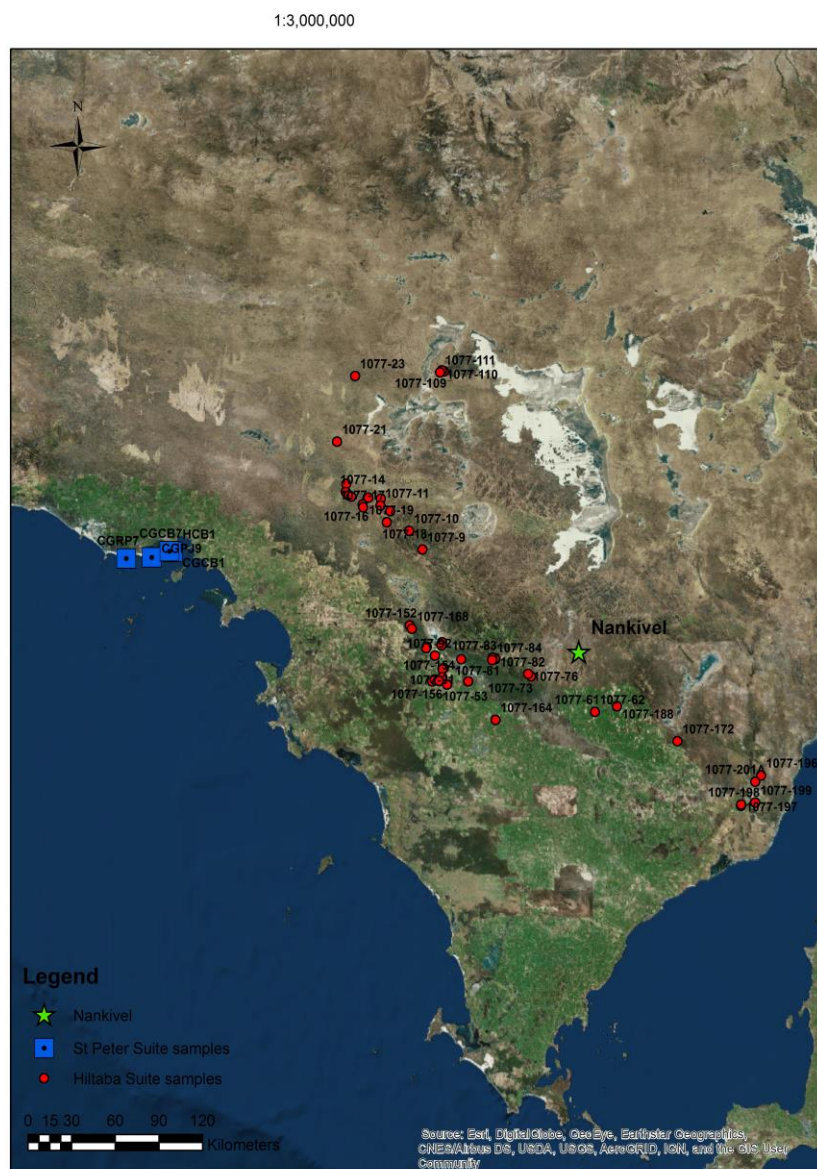


Figure 2: Sample locations with the Green star representing the Nankivel drill core.

The Olympic Iron Ore Copper Gold Province hosts the supermassive Olympic Dam Iron Ore Copper Gold deposit which is a world class deposit. the Central Gawler Gold Province is host to numerous smaller gold and silver deposits. The drill core analysed in this paper PPDH155 was drilled into the Nankivel copper gold target which is located 65km

northwest of Kimba (figure 2 map of sample locations) within the Central Gawler Gold Province with a close spatial relationship with the Paris Silver deposit. The core intersects several magmatic bodies which cover a range of silica contents and with varying degrees and types of alteration.

The collision of the St Peters Suite with the Archean Gawler nuclei is believed to have led to the initiation of the economically significant comagmatic Hiltaba suite and Gawler Range Volcanics (GRV) between 1595 and 1575 Ma (G. Swain, Barovich, Hand, Ferris, & Schwarz, 2008). Magmatic plutons are prevalent throughout much of the Gawler Craton making them one of the most spatially significant igneous bodies within the Gawler Craton (Direen & Lyons, 2007). Whilst the GRV province is constrained to the central and eastern Gawler Craton it still covers a vast spatial extent, with an approximate maximum preserved thickness of 1.5km and an areal extent greater than 25000km² it represents one of the largest examples of felsic volcanism in the world (Hand et al., 2007). With the emplacement of the Hiltaba suite magmatics extensive metalliferous enrichment is observed with the development of two key regions of economic significance, these being the Olympic Iron Ore Copper Gold (IOCG) region which hosts the supermassive Olympic Dam deposit and the central Gawler gold region (Skirrow & Davidson, 2007). Figure 3 from (Hand et al., 2007) shows the locations and spatial extents of the metalliferous regions as well as mines and prospects within them.

In this paper, the magmatic bodies intersected by drill core PPDH155 owned by investigator resources were investigated to determine the geochemical characteristics

and age of these bodies. This paper also increases the knowledge on the geological context of the Nankivel copper gold target which PPDH155 was drilled into.

Samples from the primary investigation site were provided by Investigator Resources, new geochemical analysis was also obtained for previously obtained samples from (Stewart K, 2003). The St Peter Suite data was sourced from (G. Swain et al., 2008) detailing the petrogenesis of the St Peter Suite.

After geochemical results were received it was noted that the Nankivel samples contained a number of samples which were quite mafic. As such the Nankivel data set was separated into two groups. The Mafic Nankivel data represents samples from PPDH155 with a silica content below the lowest silica content of the St Peter Suite and Hiltaba Suite samples. Whilst the standard Nankivel data labelled only as Nankivel Core in figures represents samples from PPDH155 which have a silica content above the minimum silica content observed in the St Peter Suite and Hiltaba Suite samples.

The working hypothesis of this study is that the magmatic bodies intersected in PPDH155 within the Nankivel prospect owned by Investigator resources have an age coincident with the emplacement of the 1620 – 1608 (G. Swain et al., 2008) St Peters Suite magmatics. The Null hypothesis is that the magmatic bodies are not of an age with the St Peters Suite magmatics but are coincident with the emplacement of the 1595 – 1575 (G. Swain et al., 2008) Hiltaba suite magmatics. The alternate hypothesis to these is that the magmatic bodies intersected by this drill core are comprised of products of both the St Peters Suite and the Hiltaba Suite magmatic events.

GEOLOGICAL SETTING

The Gawler Craton is located in South Australia and underwent approximately 1.7 billion years of tectonic and thermal development spanning from 3200 Ma to 1500 Ma, as such the tectonic history preserved within is highly complex (Reid & Hand, 2012).

The oldest preserved unit is the Cooyerdoo Granite (Fraser, McAvaney, Neumann, Szpunar, & Reid, 2010), The Cooyerdoo Granite is the Archean basement to the Gawler Craton where it outcrops on eastern margin.

Following the emplacement of the Cooyerdoo Granite there is no preserved record of significant tectonic or thermal activity until bimodal magmatism at 2560 – 2470 Ma which was terminated by the Sleafodian orogeny 2465 – 2410 Ma (Reid & Hand, 2012). Following this orogeny extensive basin formation and sedimentation occurred.

The 1730 – 1690 Ma Kimban orogeny reworked the Archean basement and sedimentary basins in a transpressional orogenic environment leading to the development of the structural configuration of the eastern Gawler Craton including the Kalinjala shear zone (Hand et al., 2007). Another large scale structural shear created by the dextral transpression of the Kimban orogeny was the Tallacootra shear zone which is approximately 400km long in the western Gawler Craton (G. M. Swain, Hand, Teasdale, Rutherford, & Clark, 2005). The Kimban orogeny also lead to the emplacement of large volumes of felsic and mafic magmatics (Hand et al., 2007).

Following the Kimban orogeny high temperatures are associated with the Ooldean event that occurs between 1660 and 1630 Ma, with some coeval volcanism. This event is poorly constrained spatially (Hand et al., 2007).

From 1620 – 1608 Ma the emplacement of the St Peters suite occurs having a spatial extent that covers much of the southwestern Gawler Craton and is associated with the development of a subduction zone with a debated orientation. Within this suite there are plutonic intermediate, mafic and felsic bodies with subduction-related arc-like characteristics (G. Swain et al., 2008). The St Peters suite produces a juvenile geochemical signature with ϵ_{Nd} values of -0.8 to +3.7 (G. Swain et al., 2008). The cessation of the St Peters suite magmatic event is believed to be caused by the collision of the St Peters Suite with the Archean Gawler nuclei (G. Swain et al., 2008).

METHODS

Samples were initially selected from Investigator Resources with the ones visually determined as those believed to be the least altered rocks within the core that preserved the original magmatic bodies emplaced at the site. Following this samples from the Hiltaba Suite and St Peter Suite were selected to be analysed to attempt to apply a geochemical constraint on the emplacement of the igneous bodies intersected. As such the Hiltaba Suite bodies which were selected were ones that were located in close proximity and those that had been intersected within the Central Gawler Gold Province. Whereas, the St Peter Suite samples were selected due to the quality of the data as little currently exists within the literature as outcrops of St Peter Suite rocks are limited.

Geochemical analyses were carried out on all samples obtained as minimum 30 gram rock pulp samples at Bureau Veritas Minerals in Western Australia. Samples were prepared at the University of Adelaide by processing segments of drill core through the jaw crusher cleaning the machine between each run to reduce the risk of sample contamination. Following this the rock splits were then run through the university's tungsten carbide disc mill to further crush the samples with the machinery being cleaned between each run. At this point samples for geochronology were then processed through the sieve shaker with the mesh being replaced and the equipment cleaned in between each run. Samples being prepared for processing at Bureau Veritas Minerals were crushed to rock pulp in a tungsten carbide ring mill with the equipment being cleaned between each run. The analyses that were carried out at Bureau Veritas Minerals were as follows

XRF

LA-ICP-MS

Fire Collection ICP-MS

FeO analysis.

Geochronological analysis was carried out on zircons from 4 samples of PPDH155 which were visually determined to be least altered magmatic samples. Zircons were obtained by crushing solid samples in the jaw crusher with the splits then being further crushed in the disk mill. The resulting rock chips were then separated in a sieve shaker with the fine fraction being used for mineral separation.

Mineral separation was done through panning and magnetic separation using a neodymium magnet. The zircons were then prepared and mounted to round grain

mounts. Back scattered and Cathode Luminescence Imaging (CL) was then undertaken at Adelaide Microscopy using the Quanta 600 SEM. Using the CL images 20µm spots were then selected for laser ablation using an Agilent 7500cx New Wave laser ablation system for both U/Pb dating and zircon geochemistry.

Two samples selected for Geochronology yielded enough zircons for age dating whilst the other 2 samples produced too few zircons to analyse.

Geochronological and zircon geochemistry raw data was reduced using the iolite software and then concordia plots were created using isoplot software.

Geochemical data was reduced using GCDkit (Janoušek, Farrow, & Erban, 2006) to produce Harker, Spider, Rare Earth Element and IUGS Classification plots.

**OBSERVATIONS
AND RESULTS**

The core samples that were obtained from drill hole PPDH155 were logged in figure 3 as well as containing basic observations on the rocks from prior to and during crushing, also contained within figure 3 is the information as to which reference photo found in the supplementary information is associated with each sample. It can be seen

Sample Number	From	To	Photo/ Figure	Petrology
435999	424.58	425.35	1	Qtz monzonite - Medium grained, prismatic cream coloured feldspars. High amounts of dark ferromagnesian minerals, shows low to moderate alteration
436000	404.62	405.03	2	Qtz monzonite - Medium grained, prismatic cream coloured feldspars. High amounts of dark ferromagnesian minerals, shows moderate alteration with ferromagnesian minerals showing green
436001	388.36	388.8	3	Qtz monzonite - Medium to fine grained, dark textured rock shows moderate alteration with numerous veins and ferromagnesian minerals altered to green
436002	378.9	379.16	4	Qtz monzonite - Medium grained higher amounts of potassium feldspars, pinker in colour. Shows dark veining and minor to moderate alteration
436003	360	360.34	5	Qtz monzonite - medium to fine grained, dark textured rock shows moderate alteration with numerous veins and ferromagnesian minerals altered to green also shows prismatic feldspars
436004	345.08	345.48	6	Granite - Medium grained grey to pink coloured rock, shows some evidence of minor alteration
436005	334.18	334.32	7	Granite - Medium to coarse grained shows prismatic feldspars, little evidence of alteration.
436006	319.17	320.17	Figure 3 b. Photo 8	Granite - Medium to coarse grained shows prismatic feldspars, with evidence of alteration, veins and discolouration within the crystals is evident.
436007	308.5	308.9	9	Granite - Fine to medium grained, large amounts of feldspar evident
436008	299.68	300.1	10	Granite - Medium grained altered granite fractures are evident with infilling of alteration minerals.
436009	296.35	296.67	10	Granodiorite - Fine grained altered granodiorite, larger dark coloured crystals dispersed through feldspars alteration is apparent with several fractures running through this piece of core.
436010	289	289.35	11	Granite - Medium grained appears yellow to pink with some phenocrysts of dark minerals, the feldspars appear somewhat blocky.
436011	281.68	282	12	Granodiorite - Medium grained, highly altered external surface shows as a dark to yellow colour, once broken this sample showed large amounts of euhedral pyrite.
436012	198.76	199.18	12	Syenite - Fine grained heavily altered, grey colour large amounts of pyrite along fractures also shows veining
436013	192.87	193.11	13	Qtz monzodiorite - Fine grained grey to yellow with prismatic feldspars and pyrite infilling fractures. Shows evidence of moderate alteration
436014	183.56 - 183.76	184.56 - 185	14	Qtz monzonite - Medium to coarse grained grey coloured rock with prismatic feldspars evidence of alteration with fractures showing alteration halos
436015	169.24	169.6	15	Qtz monzodiorite - Fine grained black colouration with numerous veins and fractures, pyrite is infilling space along these veins and fractures.
436016	162.4	162.68	16	Qtz monzodiorite - Fine grained brown with fractures less obvious feldspars.
436017	160.68	161	17	Qtz monzonite - Medium to Fine grained dark colouration with numerous fractures and veins moderately to heavily altered.
436018	157.22	157.58	17	Qtz monzonite - Fine grained with ferromagnesian phenocrysts appears to be heavily altered.
436019	146	146.3	18	Qtz monzodiorite - Fine to medium grained, appears to be heavily altered and brecciated with fragments of might coloured material within the overall darker rock
436020	135.33	135.67	19	Tonalite - Fine to medium grained yellow colour appears to be heavily altered, euhedral pyrite is seen throughout as well as numerous veins.
436021	119.75	120.15	20	Tonalite - Fine to medium grained yellow colour appears to be heavily altered, euhedral pyrite is seen throughout as well as numerous veins.
436022	111	112	21	Tonalite - Fine to medium grained yellow colour appears to be heavily altered, euhedral pyrite is seen throughout as well as numerous veins. Euhedral quartz is also visible in this sample.
436023	107.74	108.22	Figure 3 c. Photo 21	Tonalite - Fine to medium grained ranging from grey to yellow shows heavy veining with pyrite associated with the veins.
436024	60.4	60.85	Figure 3 a. photo 22	Qtz monzodiorite - Medium grained, prismatic cream feldspars and dark ferromagnesian minerals with some veining and discoloration.

Figure 3: core log and petrographical observations

that throughout the core significant alteration has occurred to the magmatic bodies with

veining present throughout much of the core as well as the alteration of many of the minerals associated with the emplacement of these magmatic bodies.

The samples provided (figure 4) show the range of magmatic rocks which were analysed from this site, figure 4a displaying the most mafic sample, figure 4b shows an intermediate sample which was used as a geochronological sample and figure 4c shows the most felsic sample. Also included in figure 4 are thin section photomicrographs from the core figure 4d shows a potassic altered monzodiorite with a microbrecciation band. Relict biotite is evident as larger red/brown plates as opposed to the alteration biotite which appears as fine bright

specks. Figure 4e shows a fragment of strongly altered granitoid wall rock hosted in breccia with the altered granitoid being bottom right of the photomicrograph below the

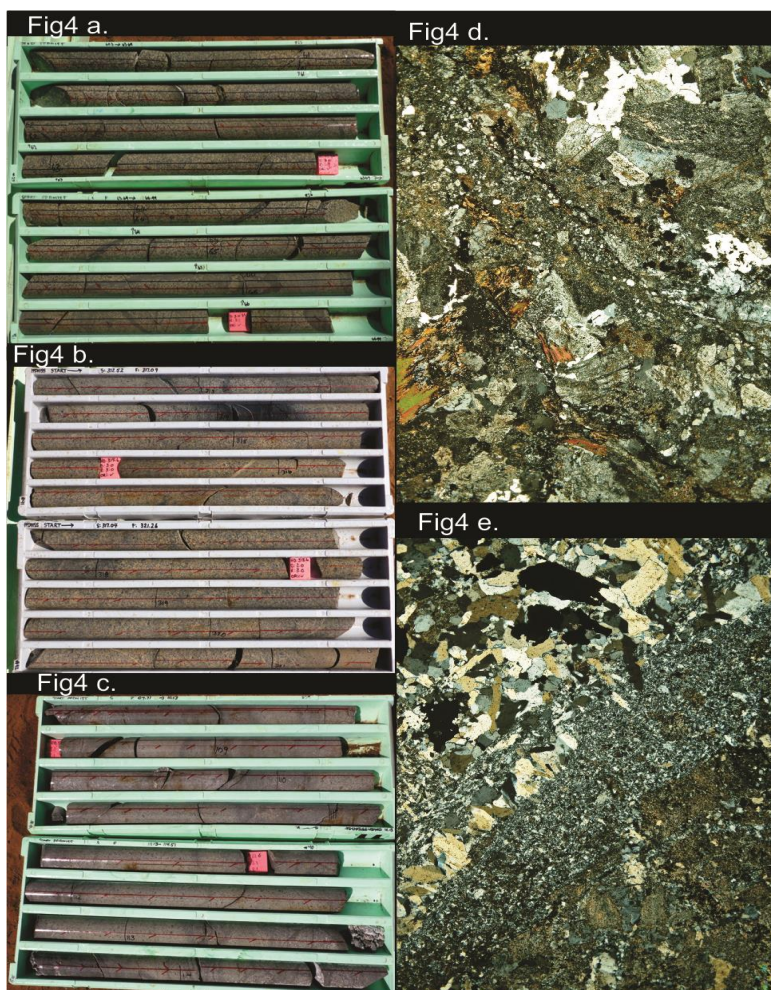


Figure 4: PPDH155 Core photos and thin section photomicrographs. 4a) Core photo of 60.3m – 66.99m segment containing sample 436024 which is the most mafic sample with silica of 55.4%. 4b) Core photo of 312.52m – 321.26m segment containing sample 436006 which is an intermediate sample with silica of 64.6%. 4c) Core photo of 107.71m – 114.51m segment containing sample 436023 which is the most felsic sample with silica of 69.5%. 4d) Photomicrograph of cross polarised sample at 369.7m showing potassic alteration of quartz monzodiorite with relict biotites as large red/brown plates. 4e) Photomicrograph of cross polarised sample at 247.47m – 247.80m showing granitoid wall rock fragment hosted in breccia, granite is to the bottom right of the image.

All Images in this figure provided by Investigator resources

grey band. Larger images of these samples are available in the appendix. Visible in these images are evidence of alteration that has occurred to the magmatic bodies with all samples showing significant evidence of large amounts of fluid migration as veins and alteration halos.

Geochemical analysis was obtained as per the methods section and the unprocessed data obtained is available for viewing in the appendix. This data was then processed using GCDkit. Figure 5 shows the IUGS rock classification obtained for the samples using the total alkali system proposed by Middlemost 1985 (J. B. H, 2009). As can be

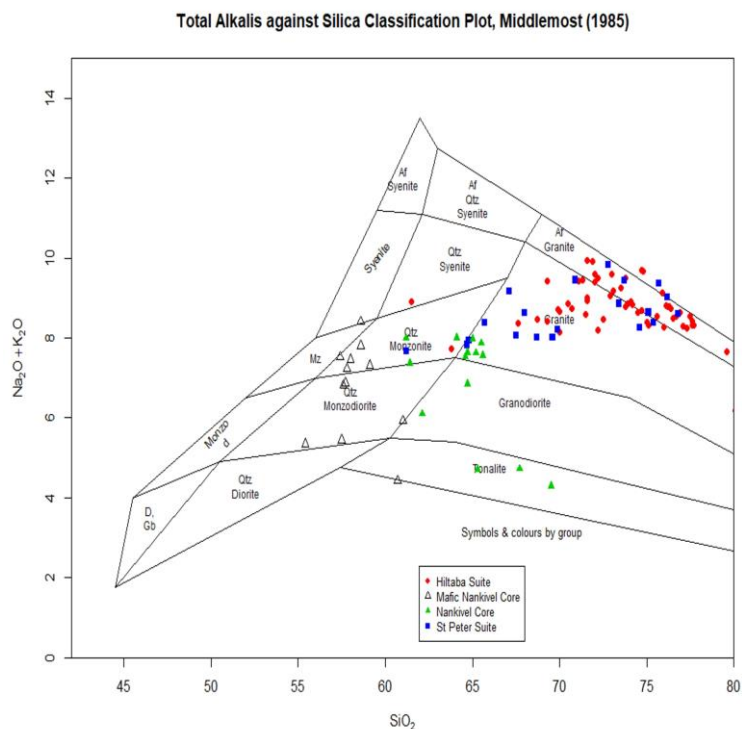


Figure 5: IUGS output from GCDkit using the TAS system from Middlemost 1985 (J. B. H, 2009)

seen the Hiltaba Suite and St Peter Suite rocks being analysed fall within the monzonite, quartz monzonite and granite fields. However, the samples from drill core PPDH155 show a much greater spread in composition. The mafic Nankivel samples are identified as monzodiorite, monzonite, diorite and granodiorite. Whilst the Nankivel samples are interpreted to be made up of monzonite, quartz monzonites, granodiorites and granite.

To determine the age of the magmatic bodies U/Pb age dates were obtained through zircon ablation. With zircons being preferentially selected as those which show little

evidence of alteration or metamict nature such as to obtain the emplacement age rather than the age of alteration within the system.

The two samples selected for geochronology that produced usable zircons were sample 435999 located 424.58m to 425.35m downhole and sample 436006 located 319.17m to 320.17m downhole. Sample 435999 is one of the most mafic bodies analysed having a silica content of 57.4% whilst 436006 has an intermediate silica content of 64.6%.

The laser ablation data obtained was then processed through Iolite software and then refined into zircon concordia graphs seen in figure 6a and 6b with 6a showing the concordia plot for sample 436006 and 6b showing sample 435999. The age dates obtained show 1577 \pm 24 Ma and 1624 \pm 38 Ma. These dates indicate that the magmatic bodies were

emplaced around the same time as the Hiltaba Suite and St Peter Suites were

being emplaced. The zircons from 435999 were checked to ensure that there was only one population recorded there and no breaks were seen in the data.

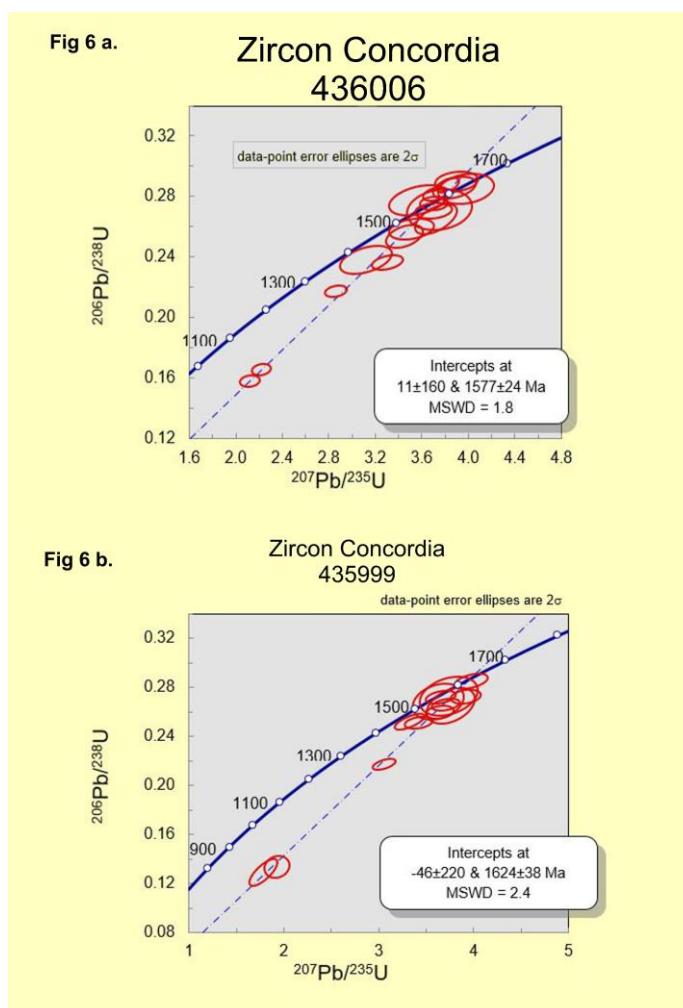


Figure 6: Zircon concordia graphs. 6a) shows sample 436006 with an age date of 1577 \pm 24 Ma. 6b) shows sample 435999 with an age date of 1624 \pm 38 Ma.

Harker diagrams

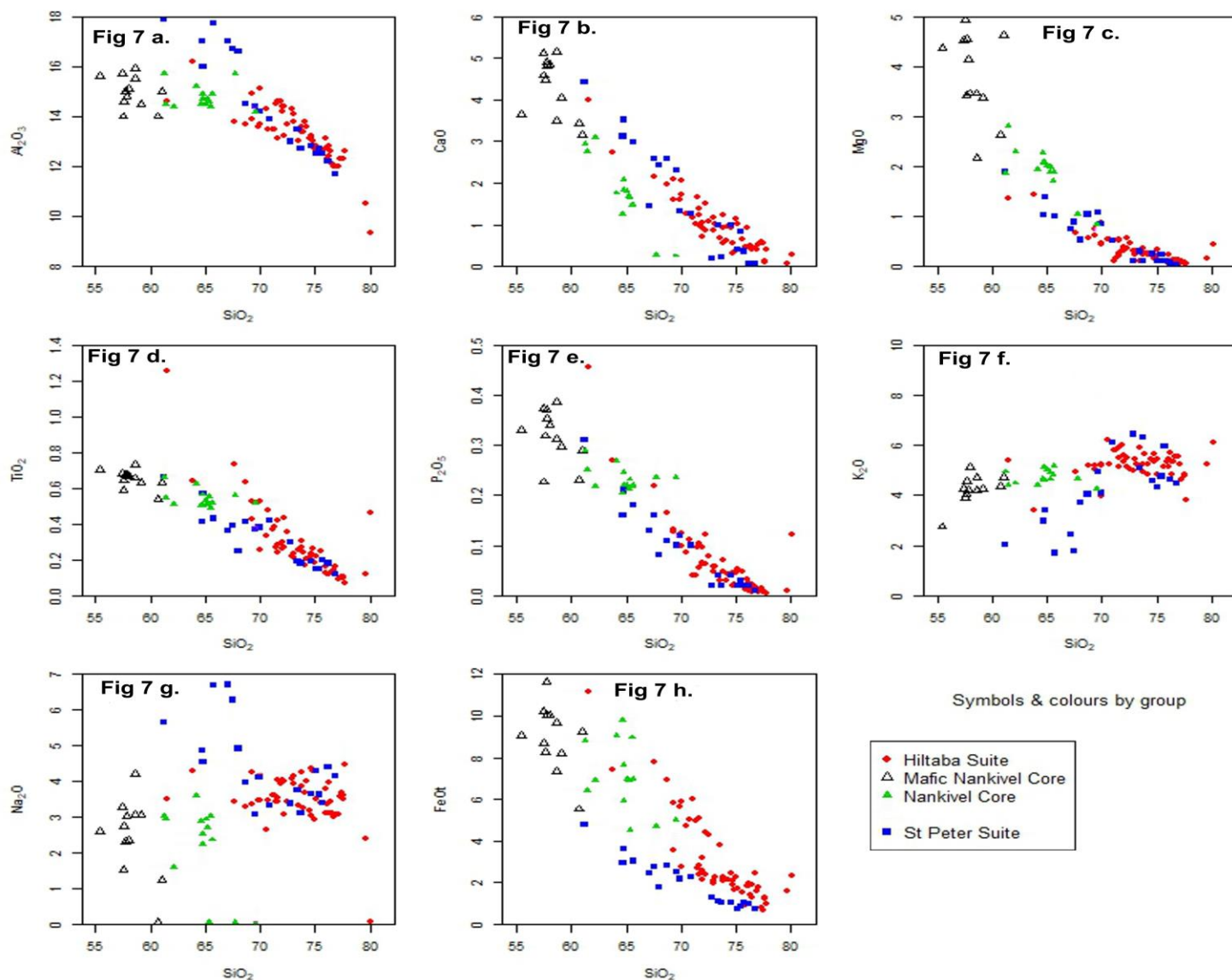


Figure 7: Harker diagrams. 7a) Al₂O₃ vs SiO₂. 7b) CaO vs SiO₂. 7c) MgO vs SiO₂. 7d) TiO₂ vs SiO₂. 7e) P₂O₅ vs SiO₂. 7f) K₂O vs SiO₂. 7g) Na₂O vs SiO₂. 7h) Fe₂O₅ vs SiO₂.

The whole rock geochemical characteristics were analysed and Harker diagrams were created to show major element trends with silica. These plots are shown in figure 7.

Several strong trends are evident with strong negative trends evident for CaO, MgO, P₂O₅, and Fe₂O₅ as shown by figures 7b, 7c, 7e, and 7h respectively. A strong negative trend is seen for the 1595 Ma Hiltaba Suite and the 1620 Ma St Peter Suite in figure 7a. However, no such trend is observed in the Nankivel samples.

A spider plot for all samples was created using GCDkit normalising to the primitive mantle values of (McDonough & Sun, 1995) this is shown in figure 8a. It is possible to

see from figure 8a that there is significant overlap of trends within this data with the St Peter Suite trend as well as the trends for both mafic and standard Nankivel being within the Hiltaba Suite Trend. It should be noted that the Nankivel samples show very little variation between the Mafic Nankivel samples and the standard Nankivel samples.

Figure 8b shows the rare earth element analysis of the samples produced in GCDkit normalised to REE chondrite values from (Boynton, 1983). This shows trends with a large range for the

Hiltaba Suite and St Peter Suite data. However, the Nankivel trends again show much

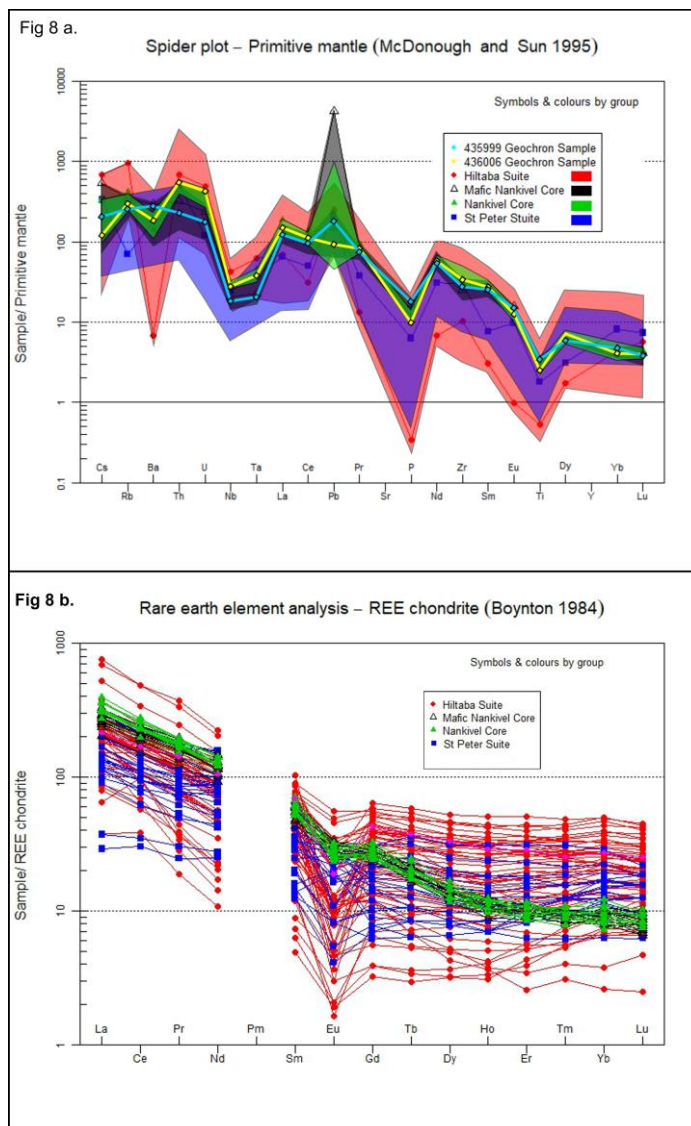


Figure 8: Spider and Rare Earth Element analysis plots. 8a) shows the ranges of values that the Hiltaba Suite, St Peter Suite and Nankivel core show when plotted in a spider plot normalised to (McDonough & Sun, 1995). It also shows the spider plot results for the 2 geochronology samples. **Figure 8b)** shows the range of data that the investigated samples returned when analysed for rare earth element data, these samples are normalised against (Boynton, 1983).

less variation as well as a less negative Eu anomaly and lesser enrichment in the heavy rare earth elements than in the Hiltaba Suite and St Peter Suite.

DISCUSSION

The age dates obtained cover both Hiltaba Suite and St Peter Suite age dates with an overlap within error ranges from 1586 Ma – 1601 Ma if the magmatic bodies are representative of a single period of magmatic emplacement it likely falls within this time frame. In addition to this a recent investigation at a location with a close spatial relationship to PPDH155 was carried out by (Nicolson et al., 2017) where age dating of advanced argillic alteration at Nankivel Hill was attempted by age dating alunite samples. The best estimate of the acid sulfate alteration event from this study was 1586 +/- 8 Ma (Nicolson et al., 2017) which correlates to Hiltaba Suite emplacement. Given the overlap of age data there is strong evidence to suggest that emplacement of at least a portion of the igneous bodies at this site are linked to the Hiltaba Suite. The evidence also shows a potential temporal relationship between emplacement of igneous bodies within PPDH155 and advanced argillic alteration at Nankivel Hill which is less than 2kms away from PPDH155.

However, it is possible that multiple episodes of magmatic emplacement have occurred at the site beginning with emplacement coincident with the St Peter Suite and continuing through the Hiltaba Suite emplacement. This is evidenced by the age date of 1624 +/- 38 Ma obtained for sample 435999 which is consistent with St Peter Suite age emplacement. However, it can be seen in figure 6b that the zircon concordia plot shows

that the age dates
obtained from
these zircons span
continuously
through St Peter
Suite and Hiltaba

Sample	Age Ma	SiO ₂ %	Al ₂ O ₃ %	Fe ₂ O ₅ %	CaO %	MgO %	TiO ₂ %	P ₂ O ₅ %	K ₂ O %
435999	1624 +/- 38	57.4	15.7	6.33	5.11	4.51	0.685	0.374	4.25
436006	1577 +/- 24	64.6	14.5	5.89	1.26	2.27	0.502	0.204	4.65
Relative % of oxide in 436006 compared to 435999		+12	-8.3	-7	-75.4	-49.7	-26.8	-45.5	+9.4

Figure 9: Major oxide values for age dated samples

Suite ages with no distinct separate populations and with Hiltaba Suite ages included within the error range for this sample which may indicate that it is solely Hiltaba. A third possible outcome of this data is that the igneous bodies at this site are genetically linked and that the bodies with an age similar to the Hiltaba Suite are products of fractional crystallisation or partial melting of material that was emplaced during the St Peter Suite emplacement period. This is supported by an increase in the silica content occurring between 1624 Ma and 1577 Ma as well as the major oxide trends seen in figure 7. Figure 9 shows a table comparing major oxide values for samples 435999 and 436006 from this we can see that the more silicic sample 436006 sees reductions in all major oxides excluding silica and K₂O with very significant reductions being seen in CaO, MgO, P₂O₅ and TiO₂. These values may have been influenced by several individual factors or a combination of them such as fractional crystallisation, new influx of magma to the system and element redistribution due to alteration. Further research is needed to investigate these relationships, the processes that occurred and the relative timing of these events.

The major oxide trends of the Hiltaba Suite, St Peter Suite and PPDH155 samples can be seen in figure 7. The trends observed are predominantly linear in nature with

decreases in percentages for all oxides with increasing silica apart from the incompatible elements K and Na. Both the Hiltaba Suite and St Peter Suite show unique features in these oxide values with the PPDH155 samples following the 1595 Ma Hiltaba Suite trend more closely. Figure 7a shows the Al_2O_3 trend with the St Peter Suite and Hiltaba Suites both showing strong negative linear relationships as silica increases. However, the PPDH155 samples show very little differentiation with increase in silica. This trend may be related to the alteration present at the Nankivel Core location. Also seen in the Nankivel Core is a strongly correlated more strongly negative trend for CaO as opposed to the trends observed in the St Peter Suite and Hiltaba Suites as seen in figure 7b. The St Peter Suite samples have characteristics in the oxide trends which differentiate them from the Hiltaba Suite and Nankivel Core samples the most obvious of these are the alkali oxide values. The oxide trend seen for Na_2O follows a moderately correlated strongly negative trend with very high starting percentages of 6.71% Na_2O as opposed to the maximum Hiltaba Suite 4.47% Na and maximum Nankivel Core 4.2% Na which both show weak correlation and very little differentiation with increase in silica content as seen in figure 7g. The St Peter Suite K_2O trend also shows as quite different from the trends seen for the Hiltaba Suite and Nankivel Core as seen in figure 7f. This is as the St Peter Suite trend increases from relatively K_2O under saturated at lower silica contents with a minimum value of 1.7% K_2O at 65.7% SiO_2 increasing strongly to a maximum value of 6.45% K_2O at 72.8% SiO_2 .

The spider and rare earth element plots shown in figure 8 show strong trends with broad ranges of values for the Hiltaba Suite and St Peter Suite data whilst the Nankivel Core data shows a strong trend with a narrow range of values. The Hiltaba Suite trend in

figure 8a starts with high values and shows several anomalies with Ba, P, and Ti and anomalously high Th and U. The Th and U anomalies are typical of the Hiltaba Suite granites. The data shows that the Hiltaba Suite samples have a broad range with a large proportion of elevated values. The St Peter Suite samples follow a similar trend in 8a however the values for these samples are moderate in comparison to the Hiltaba Suite values and lack a Th or a U anomaly. However, the Nankivel Core samples show values that are higher than the St Peter Suite data in the lighter elements as well as a much less negative Ba anomaly and with the inclusion of a Pb anomaly. The Pb anomaly is likely a feature of alteration. Figure 8b shows a much smoother trend again with very large range in the Hiltaba Suite and St Peter Suite data and much more constrained range for the Nankivel Core data. For the rare earth data, there is a large amount of overlap of data with the St Peter Suite and Nankivel Core data both lying within the range of the Hiltaba Suite data. The Hiltaba Suite rare earth trend shows two phases the first is the relatively strong negative trend until the strongly negative Eu anomaly is reached then following that the trend flattens out significantly for the High Field Strength Elements (HFSE). The St Peter Suite data follows a much flatter profile throughout with a lesser negative Eu anomaly and a weaker negative trend for the lighter rare earth elements. However, the Nankivel Core data displays a more consistent negative trend and the Eu anomaly is far smaller in comparison to the Hiltaba Suite and St Peter Suite anomalies. The Nankivel Core also appears to be much less enriched in the HFSE elements relative to the lighter rare earth elements compared with the St Peter Suite and the Hiltaba Suite. Overall the spider plot and rare earth element data for the Nankivel Core samples is shown to have a much smaller range of values than those of the Hiltaba Suite or the St Peter Suite even though the rocks are more compositionally

varied at the Nankivel Core location. There are likely several factors that influence that with the major factor being that the Nankivel Core data is from a single location whereas the data from the other suites is from a large number of locales with the second most important factor likely being the influence of element redistribution during alteration at the Nankivel Core site. Because of the large amount of overlap the Spider plot and rare earth element data does not give any definitive indication as to which suite the magmatic bodies in PPDH155 are genetically related to.

There are several aspects of the magmatic bodies intersected in PPDH155 core that warrant future investigation as a means to more closely identify the formation processes, relationships between events and bodies as well as to better constrain the age dates of the emplacement and events that led to the formation of Nankivel Copper Gold Target. As a way to better understand the relationships between the bodies and alteration apatite analysis could be undertaken in conjunction with further U/Pb dating of zircons in both the more mafic and felsic samples to attempt to identify if there is an age relationship to silica content. Another avenue of investigation which may provide useful information would be to carry out more detailed thin section petrography analysis and investigate the textural relationships between magmatic bodies and alteration.

CONCLUSIONS

Samples from Investigator Resources PPDH155 Nankivel Core were analysed using geochemical and geochronological techniques to attempt to determine their emplacement age as well as their formational conditions and relationships. Age dates of 1577 \pm 24 Ma and 1624 \pm 38 Ma were obtained for samples from PPDH155 which suggest that emplacement at least partially occurred coincident with the emplacement of

the Hiltaba Suite. The geochemistry also more closely resembles that of the Hiltaba Suite than it does the St Peter Suite when comparing the major oxide trends. However, the data also suggests that the formational processes which led to the development of these igneous bodies are quite complex and further investigation is required to produce a more detailed understanding of these processes.


ACKNOWLEDGMENTS

I would like to firstly acknowledge my supervisors Karin Barovich and Justin Payne for all of the assistance and patience that you have given me through this year. Secondly, I would like to acknowledge John Anderson and the rest of the Investigator Resources team for their support and for supplying samples and relevant information for this paper. Next, I would like to thank Juraj Farkas for his efforts as honours coordinator. I would also like to acknowledge Alec Walsh for his training and assistance throughout the year. Special thanks go to Travis Pauley for assisting with sample preparation and for helping bounce ideas around in the early days of the year. I would also like to thank Nicholas Capogreco for his hints on panning as well as Laura Morrisey and Naomi Tucker for the help with mount creation. I would also like to acknowledge Adelaide Microscopy in particular Sarah for her assistance with the laser.

REFERENCES

- Boynton, W. V. (1983). Cosmochemistry of the rare earth elements: meteorite studies. *Rare Earth Element Geochemistry*, 63-114.
- Direen, N. G., & Lyons, P. (2007). Regional Crustal Setting of Iron Oxide Cu-Au Mineral Systems of the Olympic Dam Region, South Australia: Insights from Potential-Field Modeling. *Economic Geology*, 102(8), 1397-1414. doi:10.2113/gsecongeo.102.8.1397
- Fraser, G., McAvaney, S., Neumann, N., Szpunar, M., & Reid, A. (2010). Discovery of early Mesoarchean crust in the eastern Gawler Craton, South Australia. *Precambrian Research*, 179(1-4), 1-21. doi:<https://doi.org/10.1016/j.precamres.2010.02.008>
- Hand, M., Reid, A., & Jagodzinski, L. (2007). Tectonic Framework and Evolution of the Gawler Craton, Southern Australia. *Economic Geology*, 102(8), 1377-1395. doi:10.2113/gsecongeo.102.8.1377
- J. B. H, T. (2009). *E. A. K. Middlemost 1985. Magmas and Magmatic Rocks. An Introduction to Igneous Petrology. x + 266 pp. London, New York: Longman. Price £13.95 (paperback). ISBN 0 582 30080 0 (Vol. 123).*
- Janoušek, V., Farrow, C. M., & Erban, V. (2006). Interpretation of Whole-rock Geochemical Data in Igneous Geochemistry: Introducing Geochemical Data Toolkit (GCDkit). *Journal of Petrology*, 47(6), 1255-1259. doi:10.1093/petrology/egl013
- McDonough, W. F., & Sun, S. s. (1995). The composition of the Earth. *Chemical Geology*, 120(3), 223-253. doi:[https://doi.org/10.1016/0009-2541\(94\)00140-4](https://doi.org/10.1016/0009-2541(94)00140-4)
- Nicolson, B., Reid, A., McAvaney, S., Keeling, J., Fraser, G., & Vasconcelos, P. (2017). Timing of advanced argillic alteration at Nankivel Hill, SE of Paris silver deposit, northern Eyre Peninsula. *MESA Journal*, 83(2), 20-26.
- Reid, A. J., & Hand, M. (2012). Mesoarchean to mesoproterozoic evolution of the southern Gawler Craton, South Australia. *Episodes*, 35(1), 216-225.
- Skirrow, R. G., & Davidson, G. J. (2007). A Special Issue Devoted to Proterozoic Iron Oxide Cu-Au-(U) and Gold Mineral Systems of the Gawler Craton: Preface. *Economic Geology*, 102(8), 1373-1375. doi:10.2113/gsecongeo.102.8.1373
- Stewart K, F. J. (2003). *Mesoproterozoic Granites of South Australia* (15). Retrieved from South Australia:
- Swain, G., Barovich, K., Hand, M., Ferris, G., & Schwarz, M. (2008). Petrogenesis of the St Peter Suite, southern Australia: Arc magmatism and Proterozoic crustal growth of the South Australian Craton. *Precambrian Research*, 166(1-4), 283-296. doi:<https://doi.org/10.1016/j.precamres.2007.07.028>
- Swain, G. M., Hand, M., Teasdale, J., Rutherford, L., & Clark, C. (2005). Age constraints on terrane-scale shear zones in the Gawler Craton, southern Australia. *Precambrian Research*, 139(3-4), 164-180. doi:<https://doi.org/10.1016/j.precamres.2005.06.007>

APPENDIX A: CORE PHOTOGRAPHS

Sample Number	From	To	Photo/ Figure	Photo
435999	424.58	425.35	1	 <p>The photograph shows two trays of core sample 435999. The top tray is labeled 'MINIS START' with 'S: 424.22' and 'F: 424.69'. It contains sections 4416, 4417, 4418, 4419, and 4420. The bottom tray is labeled 'MINIS START' with 'S: 424.69' and 'F: 425.21'. It contains sections 4421, 4422, 4423, 4424, and 4425. Red labels with handwritten text are attached to sections 4416, 4419, 4422, and 4425.</p>
436000	404.62	405.03	2	 <p>The photograph shows two trays of core sample 436000. The top tray is labeled 'MINIS START' with 'S: 404.62' and 'F: 404.93'. It contains sections 4400, 4401, 4402, 4403, and 4404. The bottom tray is labeled 'MINIS START' with 'S: 404.93' and 'F: 405.03'. It contains sections 4405, 4406, 4407, and 4408. Red labels with handwritten text are attached to sections 4402, 4405, and 4408.</p>

436001	388.36	388.8	3	
436002	378.9	379.16	4	
436003	360	360.34	5	

436004	345.08	345.48	6	
436005	334.18	334.32	7	
436006	319.17	320.17	Figure 4 b. Photo 8	

436007	308.5	308.9	9
--------	-------	-------	---

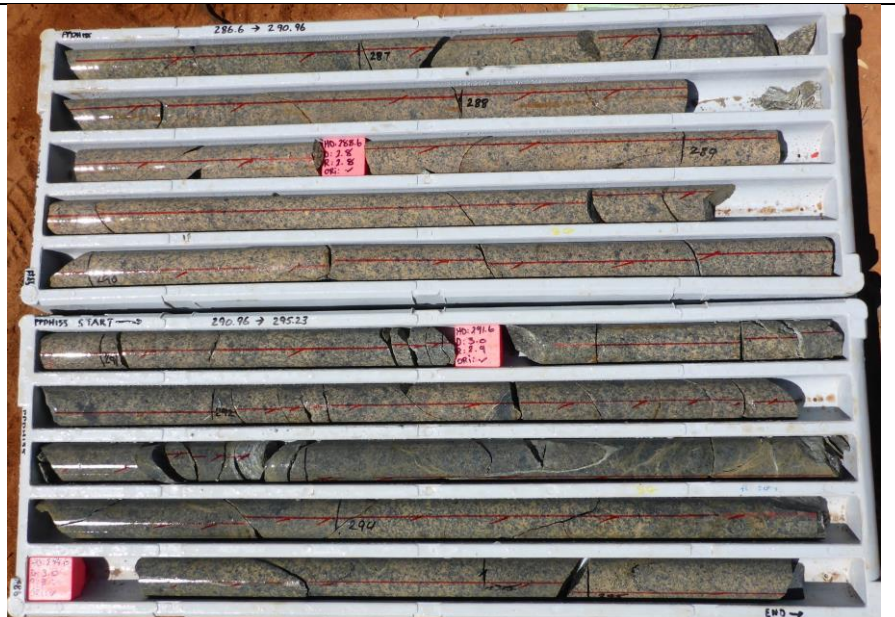


436008	299.68	300.1	10
--------	--------	-------	----






436009	296.35	296.67	10
--------	--------	--------	----


436010	289	289.35	11
--------	-----	--------	----



436011	281.68	282	12	
436012	198.76	199.18	12	
436013	192.87	193.11	13	
436014	183.56 - 183.76	184.56 -185	14	

436015	169.24	169.6	15	
436016	162.4	162.68	16	
436017	160.68	161	17	

436018	157.22	157.58	17	
436019	146	146.3	18	
436020	135.33	135.67	19	
436021	119.75	120.15	20	

436022	111	112	21	
436023	107.74	108.22	Figure 4 c. Photo 21	
436024	60.4	60.85	Figure 4 a. photo 22	